Parameter Free Driven Liouville–von Neumann Approach for Time-Dependent Electronic Transport Simulations in Open Quantum Systems – Supporting Information

Tamar Zelovich[1,*], Thorsten Hansen[2], Zhen-Fei Liu[3,4,5], Jeffrey B. Neaton[3,4,5,6], Leeor Kronik[7], and Oded Hod[1]

1) Department of Physical Chemistry, School of Chemistry, The Raymond and Beverly Sackler Faculty of Exact Sciences and The Sackler Center for Computational Molecular and Materials Science, Tel Aviv University, Tel Aviv 6997801, Israel

2) Department of Chemistry, Copenhagen University, Universitetsparken 5, DK-2100, Copenhagen Ø, Denmark

3) Department of Physics, University of California, Berkeley, Berkeley, California 94720-7300, USA

4) Materials Sciences Division, Lawrence Berkeley National Laboratory, Berkeley, California 94720, USA

5) Molecular Foundry, Lawrence Berkeley National Laboratory, Berkeley, California 94720, USA

6) Kavli Energy NanoSciences Institute at Berkeley, Berkeley, California 94720, USA

7) Department of Materials and Interfaces, Weizmann Institute of Science, Rehovoth 76100, Israel

* Present address: *Department of Chemistry, New York University, New York, NY 10003, USA*

Energy Independent Broadening Factors

A central assumption made in the derivation of the parameter-free driven Liouville von Neumann approach, described in the main text, is that the state-specific broadening factors are independent of energy. To demonstrate the validity of this assumption we have calculated the full energy dependence of these factors for a 50-site tight-binding chain lead model with onsite energies of 0 eV and nearest-neighbor hopping integrals of -0.2 eV. To this end, we have evaluated the dressed lead Hamiltonian defined in the main text using the full energy-dependent reservoir self-energy and extracted its energy dependent eigenvalues, whose imaginary parts represent the various lead state broadening factors. Fig. ure S1a presents 50 different diagrams, each corresponding to the energy dependence of the broadening factor associated with a given lead level due to the coupling to the reservoir.

Given this energy dependence, the shape of each lead level can be approximated as a Lorentzian, where the constant broadening factor is replaced by its energy dependent counterpart:[1]

$$L_l(E) = \frac{\frac{1}{2}\Gamma_l(E)}{(E-E_l)^2 + \left[\frac{1}{2}\Gamma_l(E)\right]^2}. \tag{S1}$$

Here, E_l is the position of lead level l and $\Gamma_l(E)$ its energy-dependent broadening factor.

As can be seen in Fig. ure S1a, for the model parameters used herein, the maximal broadening value achieved is ~0.02 eV, which serves as an upper limit on the lead level widths. Importantly, at this energy range around the level peak positions, all calculated broadening factors are only weakly dependent on energy. Away from the peak position the broadening factors further diminish, rendering their contribution negligible. Hence, to a good approximation, the broadening factors can be assumed to be energy independent and can be represented by their maximal value obtained at the corresponding lead state eigen-energy.

To further support this statement, we plot in Fig. ure S1b the Lorentzian function of Eq. S1 for three out of the 50 levels shown in Fig. ure S1a, with both energy dependent and constant maximal value broadening. Clearly, for the three levels considered the constant broadened and energy dependent broadened Lorentzians almost completely overlap over the entire relevant energy range, thus justifying the use of constant broadening factors for this system. The inset of Fig. ure S1b presents a zoom-in on the tail regions of the central level. It shows, as expected, that using a constant maximal value broadening (green curve) produces a slightly longer tail than using the full energy dependent broadening function (blue curve).

Another assumption made while invoking the wide band approximation in the main text involves neglecting the lead level shifts due to the coupling to the semi-infinite reservoir. To demonstrate the validity of this assumption we follow the procedure described above now considering the real-part of the reservoir self-energy, Fig. ure S1c presents the energy dependence of the entire lead eigenvalue spectrum. The results clearly demonstrate that, for the chosen model parameters, the shifts in lead level positions due to the coupling to the reservoir are negligible relative to the full lead bandwidth and smaller than the typical lead spacing. Furthermore, no level crossing occurs in the entire energy range considered. Importantly, in the vicinity of the Fermi energy (see inset) the level shifts are shown to be nearly parallel thus further justifying their neglect. As a general remark, we expect this approximation to become better with increasing lead section size.

(a)

(b)

(c)
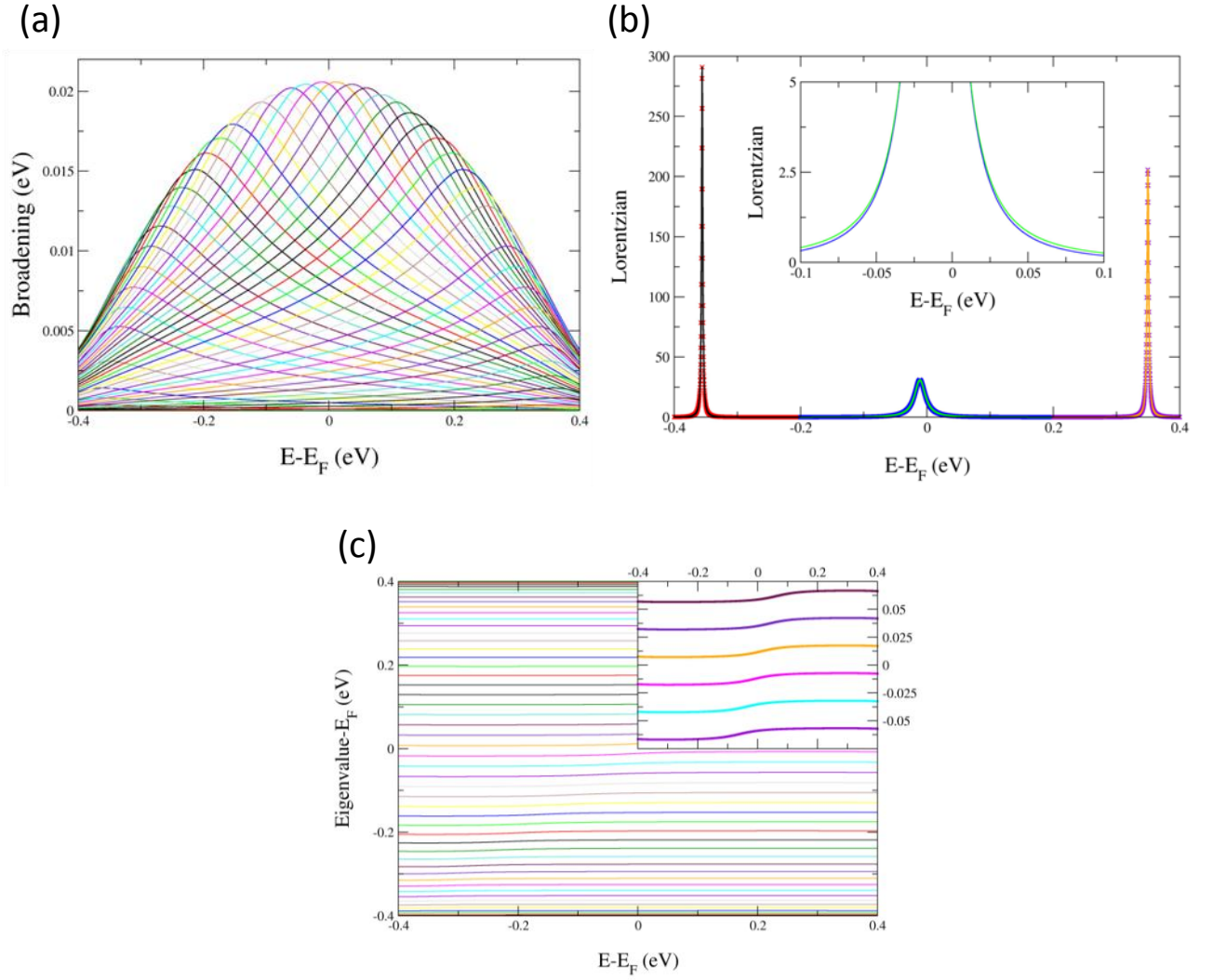
Figure S1: (a) Explicit energy dependence of the lead state-specific broadening factors for a 50-site tight-binding chain lead model with onsite energies of 0 eV and uniform nearest-neighbor hopping integrals of -0.2 eV. Each color represents the energy-dependence of a different state-specific broadening factor. (b) Lorentzian line-shapes plotted for three representative lead states using Eq. S1. Full lines represent Lorentzians having constant broadening factors, chosen as the maximal broadening of the respective state. X marks are obtained using the corresponding energy-dependent broadening functions appearing in the left panel. Inset: zoom in on the tail regions of the central Lorentzian function. (c) Explicit energy dependence of the lead level positions. Inset: zoom in on the level shifts in the vicinity of the Fermi energy.

State-Dependent Vs. Uniform Broadening

The PF-DLvN approach presented in the main text improves over the original DLvN approach[2][3][4][5] in two ways: (i) the uniform driving rate appearing in the original implementation is replaced by lead state-specific broadening factors that account more accurately for the effect of coupling the lead to the reservoir; (ii) the broadening factors are calculated explicitly from the electronic properties of the corresponding reservoir, eliminating the need for any fitting procedure. In the main text we have focused on the ability of the new methodology to capture the current dynamics and reproduce the correct steady-state current values. To enhance the understanding of the method's performance we further compare the current traces and steady-state occupations obtained using the full PF-DLvN approach with lead state-specific broadening factors and a uniform broadening factor chosen as the highest state-specific broadening obtained using the $H + \Sigma$ method for each system.

Fig. ure S2 compares the PF-DLvN current trace (black), obtained for the tight-binding junction model considered in the main text, to the uniform driving rate trace (red). The two method provide very similar current traces that reproduce the Landauer steady-state current. The steady-state occupations of the left (full lines) and right (dashed lines) leads resemble their target values (blue) with minor deviations within the Fermi transport window region (see inset of Fig. ure S2), indicating that the leads are not fully driven to their equilibrium value. This has a minor effect on steady-state occupations of the molecular section (circles and '+' signs)[2], which are found to be very similar in both methods.

Using a single driving rate, whose value is the maximal lead state-specific broadening, for the hydrogen chain bridging two finite width hydrogen lead models, produces current traces very similar to those obtained by the full PF-DLvN approach (see Fig. ure S3). The lead steady-state occupations obtained by the two approaches (see inset of Fig. ure S3) follow their target values in a very similar manner. The corresponding occupations of the molecular states are widely scattered, reflecting their asymmetric coupling to the lead states within the extended Hückel electronic structure treatment.[3][4] Interestingly, the uniform broadening molecular occupations deviate from the full PF-DLvN values throughout the Fermi transport region but with minor effect on the steady-state current.

When applying both methods to the carbon atomic chain junction model at the extended Hückel level of theory, the current traces deviate from each other. The uniform driving rate current is consistently smaller than that obtained using the full PF-DLvN approach (see Fig. ure S4). This is also reflected in the steady-state occupations, where the uniform driving rate typically provides lower values for the molecular occupations and smaller deviations of the lead occupations from their target values (see inset of Fig. ure S4). This indicates that the uniform driving rate, chosen as the maximal state-dependent broadening value, is too high, resulting in suppression of the current within the molecular region.[6]

When considering more realistic lead models, strongly non-uniform densities of states in the vicinity of the Fermi energy are often encountered.[4] In such cases, uniform broadening cannot be used to transform the discrete density of states of the finite lead model into the corresponding continuous counterpart. Hence, the full set of state-specific broadening factors should be used to drive the system out of equilibrium. This involves only a minor computational overhead as most of the effort involves the extraction of the appropriate broadening values from the self-energy of the reservoir.
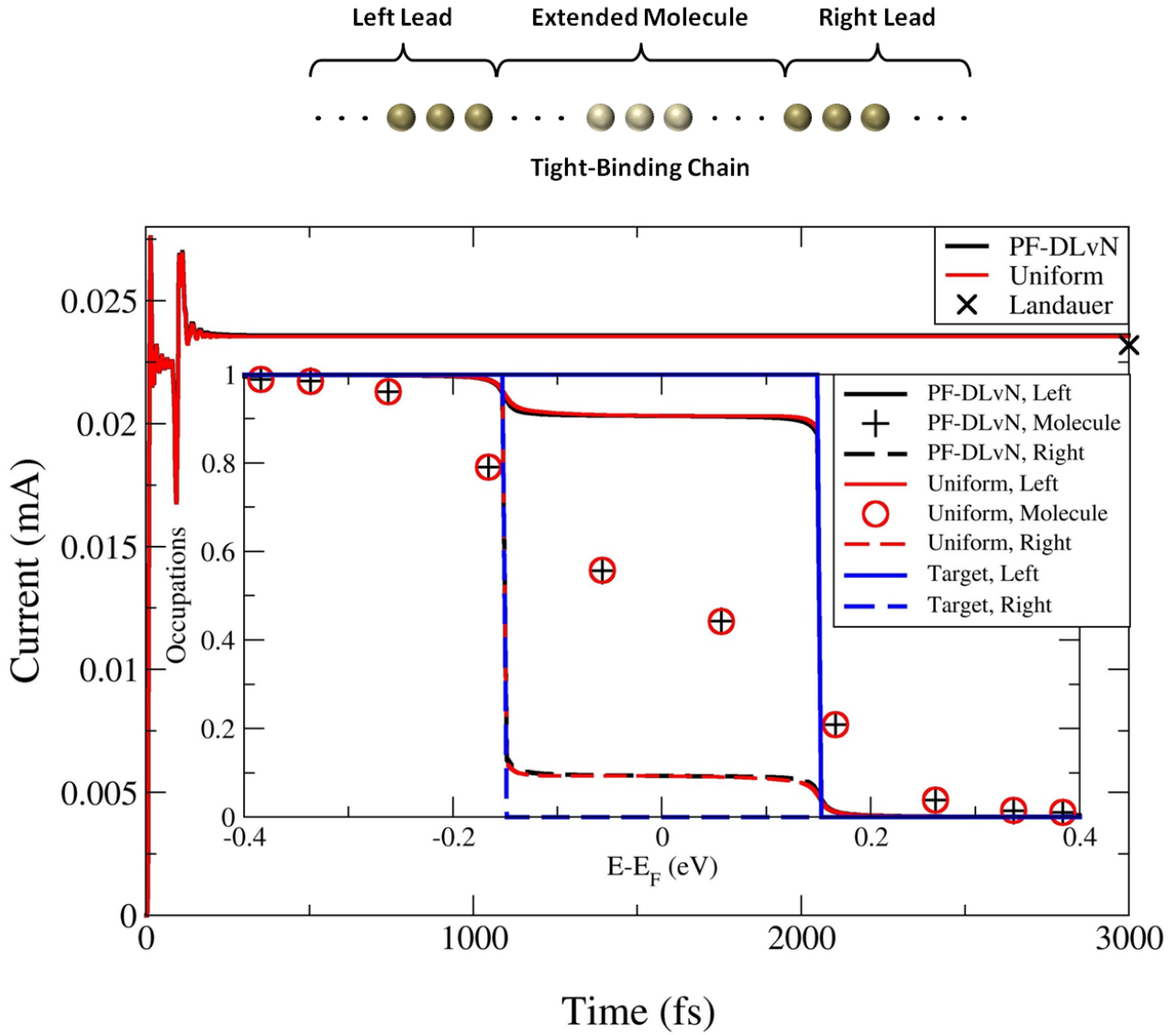
Figure S2: Comparison of the current traces (main frame) and steady-state occupations (inset) of a tight-binding chain model junction (upper illustration), obtained using the full PF-DLvN approach with state-specific broadening factors (black) and uniform broadening (red), with the latter taken as the highest calculated state-dependent broadening value (0.0057 eV). Landauer steady-state current, calculated using the procedure detailed in Ref. [2], is presented by the x mark. The inset shows the steady-state occupations of the molecular section (circles and '+' signs), and of the left (full line) and right (dashed line) leads. The corresponding target lead occupations are shown in blue. Parameters are identical to those detailed in the caption of Fig. 2b of the main text for a lead section size of 300 sites.
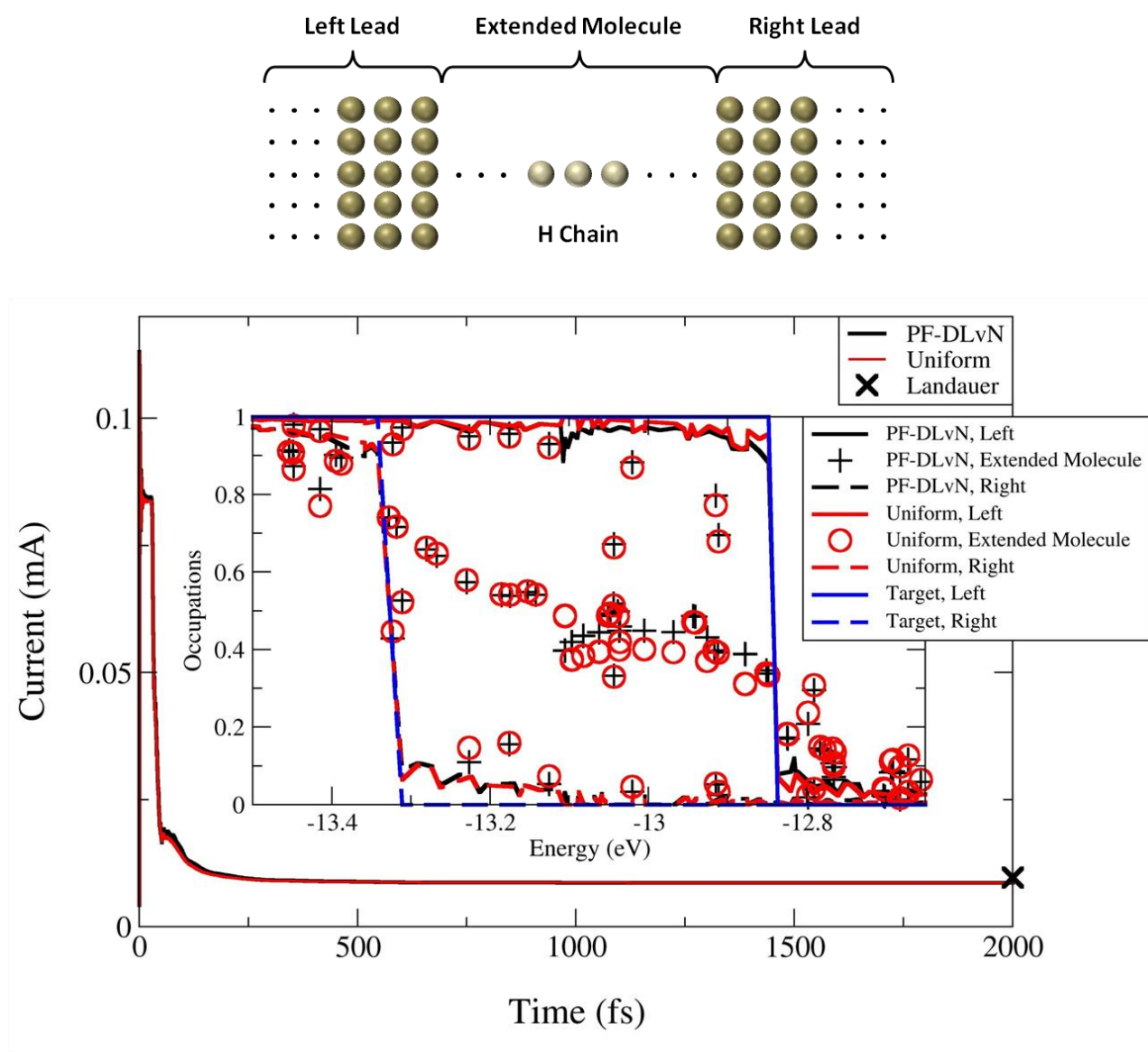
Figure S3: Comparison of the current traces (main frame) and steady-state occupations (inset) of an atomic hydrogen chain bridging two finite width hydrogen lead models (upper illustration), calculated at the extended Hückel level of theory using the full PF-DLvN approach with state-specific broadening factors (black) and uniform broadening (red), with the latter taken as the highest calculated state-dependent broadening value (0.10 eV). Landauer steady-state current, calculated using the procedure detailed in Ref. [4], is presented by the x mark. The inset shows the steady-state occupations of the extended molecule section (circles and '+' signs), and of the left (full line) and right (dashed line) leads. The corresponding target lead occupations are shown in blue. Parameters are identical to those detailed in the caption of Fig. 3b of the main text.
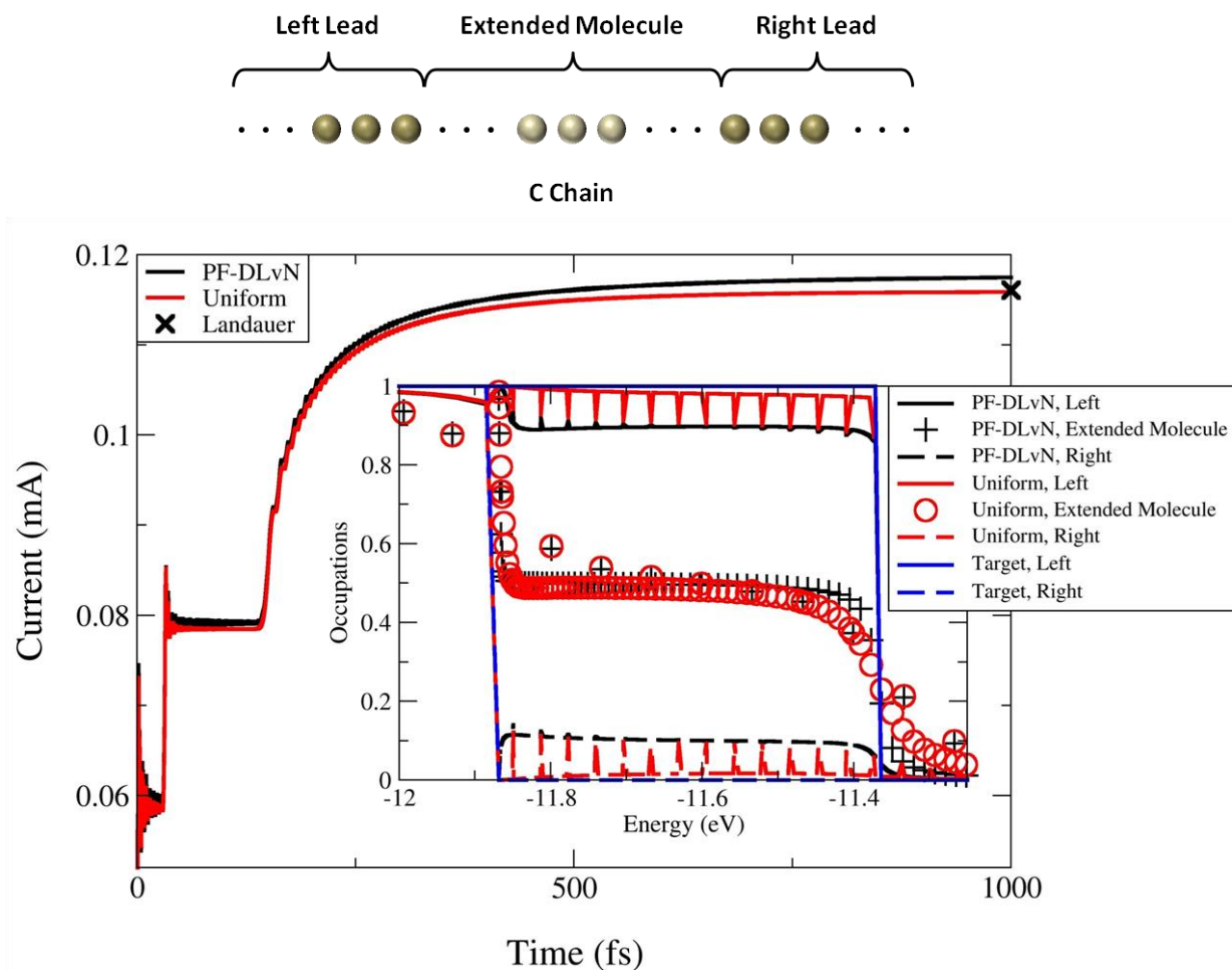
Figure S4: Comparison of the current traces (main frame) and steady-state occupations (inset) of an atomic carbon chain junction model (upper illustration), calculated at the extended Hückel level of theory using the full PF-DLvN approach with state-specific broadening factors (black) and uniform broadening (red), with the latter taken as the highest calculated state-dependent broadening value (0.063 eV). Landauer steady-state current, calculated using the procedure detailed in Ref.[4], is presented by the x mark. The inset shows the steady-state occupations of the extended molecule section (circles and '+' signs), and of the left (full line) and right (dashed line) leads. The corresponding target lead occupations are shown in blue. Parameters are identical to those detailed in the caption of Fig. 4 of the main text.

Assessment of sensitivity to η

An essential step in the calculation of the state-dependent broadening factors is the evaluation of the bare reservoir's surface Green's function (GF). To this end, in the present study we have adopted the iterative principal layer scheme of Sancho *et al.*[7][8][9][10] In this approach a small real positive parameter, η, is introduced to soften the singularities of the bare principal layer GF used during the iterative construction of the entire surface GF. Formally, η should approach zero from above ($\eta \rightarrow 0^+$). In practice, due to the finite size of the principal layer model a finite η value should be used. Typically, there exists a wide range where the calculated surface GF, and hence all other extracted physical observables, are insensitive to the value of η. Below this range, too small η values result in noticeable numerical instabilities. Above this range the surface GF becomes sensitive to the particular choice of η.

Fig. S5 presents the calculated state-dependent broadening factors as a function of single-particle state-energy, obtained using four values of η for the 200 sites one-dimensional tight-binding lead model (panel a) and 300 hydrogen atoms extended Hückel chain lead model (panel b). In both cases, the highest η value chosen provides unconverged state-dependent broadening factors. Below this value the broadening factors converge and remain stable over a few orders of magnitude of η variations. For the lowest η value shown the calculated broadening factors develop numerical instabilities, whose severity further increases with growing η.
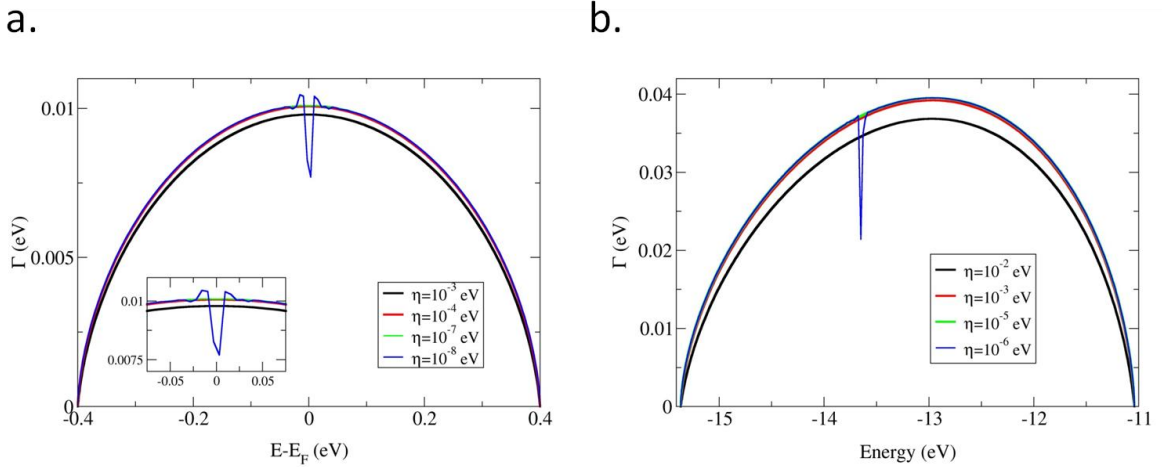
Figure S5: η sensitivity of the state-dependent broadening factors calculated for (a) the 200 sites one-dimensional tight-binding lead model and (b) the 300 hydrogen chain extended Hückel lead model. All parameters of the two lead models are provided in the main text.

In our simulations, we check for stability of the calculated state-dependent broadening factors with respect to the value of η. The broadenings that are obtained with the smallest η value that still provides numerical stability are used to perform the dynamic calculations. Importantly, this stability test needs to be performed only once per lead model and is transferable to any junction that uses the same lead. The values of η used in the different calculations can be found in the table below:

Lead model	200 sites tight-binding chain (Fig. 2)	300 sites tight-binding chain (Fig. 2)	300 hydrogen atoms extended Hückel chain (Fig.3)	500 hydrogen atoms extended Hückel finite width (Fig.3)	200 carbon atoms extended Hückel chain (Fig. 4)
η (eV)	10^{-7}	10^{-7}	10^{-4}	10^{-3}	10^{-4}

References

[1]   Z. F. Liu and J. B. Neaton, "Communication: Energy-dependent resonance broadening in symmetric and asymmetric molecular junctions from an ab initio non-equilibrium Green's function approach," *J. Chem. Phys.*, vol. 141, no. 13, 2014.

[2]   T. Zelovich, L. Kronik, and O. Hod, "State representation approach for atomistic time-dependent transport calculations in molecular junctions," *J. Chem. Theory Comput.*, vol. 10, no. 8, pp. 2927–2941, 2014.

[3]   T. Zelovich, L. Kronik, and O. Hod, "Molecule-Lead Coupling at Molecular Junctions: Relation between the Real- and State-Space Perspectives," *J. Chem. Theory Comput.*, vol. 11, no. 10, pp. 4861–4869, 2015.

[4]   T. Zelovich, L. Kronik, and O. Hod, "Driven Liouville von Neumann Approach for Time-Dependent Electronic Transport Calculations in a Nonorthogonal Basis-Set Representation," *J. Phys. Chem. C*, vol. 120, no. 28, pp. 15052–15062, 2016.

[5]   O. Hod, C. A. Rodríguez-Rosario, T. Zelovich, and T. Frauenheim, "Driven Liouville von Neumann Equation in Lindblad Form," *J. Phys. Chem. A*, vol. 120, no. 19, pp. 3278–3285, 2016.

[6]   J. E. Subotnik, T. Hansen, M. a Ratner, and A. Nitzan, "Nonequilibrium steady state transport via the reduced density matrix operator.," *J. Chem. Phys.*, vol. 130, no. May, p. 144105, 2009.

[7]   M. P. L. Sancho, J. M. L. Sancho, and J. Rubio, "Quick iterative scheme for the calculation of transfer matrices: application to Mo (100)," *J. Phys. F Met. Phys.*, vol. 14, no. 5, pp. 1205–1215, 1984.

[8]   M. P. L. Sancho, J. M. L. Sancho, J. M. L. Sancho, and J. Rubio, "Highly convergent schemes for the calculation of bulk and surface Green functions," *J. Phys. F Met. Phys.*, vol. 15, no. 4, pp. 851–858, 1984.

[9]   M. P. L. Sancho *et al.*, "A nonorthogonal-basis calculation of the spectral density of surface states for the (100) and (110) faces of tungsten," *J. Phys. C Solid State Phys*, vol. 18, no. 1, pp. 1803–1815, 1985.

[10]   M. B. Nardelli, "Electronic transport in extended systems: Application to carbon nanotubes," *Phys. Rev. B*, vol. 60, no. 11, pp. 7828–7833, 1999.